

# Synergistic Effect of Platelet-rich Fibrin Releasate and Bone Marrow Stem Cells in Preventing Bone Loss in Ovariectomized Mouse

chin chean wong

Taipei Medical University <https://orcid.org/0000-0001-6944-5241>

Jeng-Hao Liao

National Taiwan University School of Veterinary Medicine

Shi-Yuan Sheu

Chung Shan Medical University

Po-Yu Lin

National Taiwan University School of Veterinary Medicine

Chih-Hwa Chen

Taipei Medical University

Tzong-Fu Kuo (✉ [tzongfu@asia.edu.tw](mailto:tzongfu@asia.edu.tw))

---

## Research article

**Keywords:** Bone marrow, Osteoporosis, platelet-rich fibrin, releasates, stem cell

**Posted Date:** May 18th, 2020

**DOI:** <https://doi.org/10.21203/rs.3.rs-27529/v1>

**License:**  This work is licensed under a Creative Commons Attribution 4.0 International License.

[Read Full License](#)

---

**Version of Record:** A version of this preprint was published on August 8th, 2020. See the published version at <https://doi.org/10.1186/s12891-020-03549-y>.

# Abstract

**Background:** Osteoporosis is a metabolic bone disorder characterized by deterioration in the quantity and quality of bone tissue, with a consequent increase susceptibility to fracture.

**Methods:** In this study, we sought to determine the efficacy of platelet-rich fibrin releasate (PRFr) in augmenting the therapeutic effects of stem cell-based therapy in treating osteoporotic bone disorder. An osteoporosis mouse model was established through bilateral ovariectomy on 12 week-old female ICR (Institute of Cancer Research) mice. Eight weeks postoperatively, the ovariectomized (OVX) mice were left untreated (control) or injected with PRFr, bone marrow stem cells (BMSCs), or the combination of BMSCs and PRFr. Two different injection (single versus quadruple) dosages were tested to investigate the accumulative effects of BMSCs and PRFr on bone quality.

Eight weeks after injection, the changes in tibial microstructural profiles included the percentage of bone volume versus total tissue volume (BV/TV, %), bone mineral density (BMD, g/cm<sup>3</sup>), trabecular number (Tb.N, number/mm), and trabecular separation (Tb.Sp, mm) and bony histology were analyzed.

**Results:** Postmenopausal osteoporosis model was successfully established in OVX mice, evidenced by reduced BMD, decreased BV/TV, lower Tb.N but increased Tb.Sp. Eight weeks after injection, there was no significant changes to BMD and bone trabeculae could be detected in mice that received low-dose regimen. In contrast, in mice which received 4 doses of combined PRFr and BMSCs, the BMD, BV/TV, and Tb.N increased, and the Tb.Sp decreased significantly compared to untreated OVX mice. Moreover, the histological analysis showed the trabecular spacing become narrower in OVX-mice treated with high-dose injection of BMSCs and combined PRFr and BMSCs than untreated control.

**Conclusion:** The systemic administration of combined BMSCs and PRFr protected against OVX-induced bone mass loss in mice. Moreover, the improvement of bony profile scores in quadruple injection group is better than the single-injection group, probably through the increase in effect size of cells and growth factors. Our data also revealed the combination therapy of BMSCs and PRFr has a synergistic effect in enhancing osteogenesis, which may provide insight for the development of a novel therapeutic strategy in osteoporosis treatment.

## Background

Osteoporosis is a systemic skeletal disease characterized by low bone mineral density (BMD) and impaired bone microarchitecture [1]. As a consequence, an increased risk of fractures, in particular hip, spine, and wrist would occur in osteoporotic patients who sustained low energy injury [2]. Throughout life, bones are in dynamic equilibrium, meaning that they are continuously remodeled by osteoclast-mediated bone resorption and osteoblast-mediated bone formation [3]. However, the disruption of equilibrium of bone remodeling would happen when the bone-forming osteoblasts activity is surpassed by osteoclast-mediated bone resorption thereby contributes to the pathogenesis in osteoporosis [4–7]. The current medications for osteoporosis can be categorized into either antiresorptive drugs (i.e., bisphosphonates,

estrogen agonist/ antagonists, estrogens, calcitonin, and denosumab) or anabolic agent (i.e., teriparatide) [1]. Although current evidences have shown encouraging results of both types of drugs in improving BMD and reducing fracture risk, there are growing concerns about devastating drug-related complications such as osteonecrosis of jaw and atypical femoral fractures [8–10].

Osteogenesis and bone remodeling are complex processes that involve the interactions between distinct cell populations, not only the osteoblastic and osteoclastic lineages, but also an interplay between progenitor stem cells, hematopoietic and immune cells [11]. Despite the complex nature of the pathogenesis of osteoporosis, osteoblast undoubtedly play a key role in disease's pathogenesis via participating in the bone forming process. On the other hand, accumulating evidence has revealed an association of a stem cell population, derived from bone marrow in bone maintenance and remodeling [11]. Under physiological conditions, the bone tissue homeostasis is maintained through the balance between the osteogenic and adipogenic abilities of the stem cells. The dysfunction of bone marrow stem cells (BMSCs) attributed to menopause, aging or ovariectomy would therefore impair their proliferative response and osteogenic differentiation abilities [12], resulting in bone mass loss and osteoporosis [13]. From this standpoint, it would be plausible to develop the stem cell transplantation and cell-based therapies as a therapeutic strategy to provide the osteoblastic niche in order to reverse the shift towards bone resorption in osteoporosis.

Platelet-rich plasma (PRP) is a platelet concentrate derived from autologous blood and was effective in promoting proliferation and osteogenic activity of BMSCs and osteoblasts [14–16]. Unlike PRP, platelet-rich fibrin (PRF) is a gel-like platelet concentrate yielded by natural polymerization process during centrifugation without additives such as thrombin, calcium chloride or anticoagulants [17–19]. Its fibrin microarchitecture is beneficial for the containment and sustained release of growth factors over time [20]. Furthermore, the PRF releasate (PRFr) is a supernatant rich in growth factors which is separated from PRF gel through the process of quiescence and centrifugation. In previous report, PRFr could induce human mesenchymal stem cells osteogenic differentiation as characterized by the formation of calcium ossificates, increased alkaline phosphatase activity and upregulation of osteogenic markers [21]. However, the effects of PRFr and BMSCs or their combinatory use in osteoporotic treatment remained largely unknown and need to be elucidated.

In this study, we intend to explore the potential of the novel application of BMSCs and PRFr in preventing bone loss using osteoporotic mouse model. We hypothesize that the combination therapy of BMSCs and PRFr has a synergistic effect in enhancing osteogenesis, thereby favoring bone formation and ameliorate osteoporosis. Micro-computer tomography (micro-CT) imaging and histology were employed to analyze bony profile changes before and after treatments. Moreover, the dose-dependent effect of each therapeutics is examined to help determining optimal treatment regimen in future clinical application.

## Methods

### Study design and ethics statement

All procedures of platelet-rich fibrin and bone marrow stem cells isolation and surgery on experimental animals were carried out according to the guide for the Care and Use of Laboratory Animals and was approved by the Institutional Animal Care and Use Committee (IACUC approval: NTU-102-EL-82; NTU-102-EL-91).

## Harvest And Cultivation Of Bone Marrow Stem Cells

Bone marrow aspirates were obtained aseptically from mouse femurs. Bone marrow specimen was collected from the disposed aspirates using a 10 mL syringe. The aspirates were immediately mixed with 0.5 mL of sodium-heparin (10000 U/mL) and diluted in equal volume of phosphate-buffered saline (PBS). The cell suspension was then fractionated on a Lymphoprep (Fisher Scientific, Goteborg, Sweden) and centrifuged at 400 *g* for 30 minutes. The interface fraction enriched with bone marrow stem cells (BMSC) was collected and plated onto a 10 cm dish containing 10 mL of  $\alpha$  Modified Eagles Medium ( $\alpha$ MEM) containing 10% of fetal bovine serum (FBS) (Gibco, Paisley, UK), and 1X P/S/A (penicillin/ streptomycin/ fungizone). After washing out non-adherent hematopoietic cells, the adherent BMSCs were cultured in 5% CO<sub>2</sub> at 37 °C with medium changed every 3 ~ 4 days. When the cells reached 80% confluence, they were trypsinized and passaged into new 10-cm dishes at a cell density of  $5 \times 10^5$  cells/ dish. The cells were sub-cultured till passage 2 (P2). P2 cells were then seeded at a cell density of  $6.5 \times 10^3$  cells/ cm<sup>2</sup> for further *in vitro* tests.

## Flow Cytometry Analysis

BMSCs were fixed with ethanol overnight at - 20 °C. Aliquots of  $5 \times 10^5$  cells were incubated with each of the fluorochrome-conjugated antibodies against a panel of cell surface markers, including CD 34 (BD 553731, Biosciences, USA), CD 45 (AB 10558, abcam, USA), CD 44 (AB 119335, abcam, USA) and CD 90 (BD 554895, BD Biosciences, USA) at 4 C°. Cells were resuspended in Con's tube (BD) containing 200  $\mu$ L of PBS/ 1% bovine serum albumin and analyzed by flow cytometry using the FACScan system (Becton Dickinson, USA).

## Preparation Of Platelet-rich Fibrin Releasates

A laboratory mouse has a circulating blood volume of about 1.5–2.5 ml (6–8% of the body weight) [22], thus it would be difficult to obtain sufficient amount of mouse blood for experimental use. Since rabbits are of the order lagomorphs similar to rodents, thus large lot sizes available from pooled rabbit donors may be an alternative blood source [23]. In this study, blood samples were collected from the New Zealand White rabbits (mean weight 3 ~ 3.5 kg) under inhalational anesthesia with isoflurane. The PRF gel was prepared using the technique described by Choukroun et al [17]. After adequate skin cleaning, disinfection and sterilization, 8 milliliters (mL) of venous blood was harvested from rabbits in sterile tubes without anticoagulant supplement, and then centrifuged at 400 *g* for 10 minutes in a DSC-200A-2

table top centrifuge (Digisystem, Laboratory Instruments Inc., New Taipei City, Taiwan). The acquired PRF gel was located between the red blood cells and the acellular plasma. The PRF gel was then transferred into 15 mL sterile centrifuge tube and was allowed to stand quiescence for 5 hours to allow PRF releasates (PRFr) formation. According to Su et al. study, the PRFr collected at 5 hours contains notably higher concentration of growth factors which would be beneficial for bone formation [24]. Later, the PRF gel was centrifuged at 3000 g for 10 minutes and the resultant PRFr located in supernatant fraction was carefully aspirated and stored at -20 °C until use.

## Cytokine assay of Platelet-rich fibrin releasate

The PRFr derived from blood samples of five different rabbits were collected for quantitation of cytokine content. The concentrations of cytokine including platelet-derived growth factor (PDGF)-AA and BB, transforming-growth factor- $\beta$  (TGF- $\beta$ ), and bone morphogenetic protein-2 (BMP-2) were measured using commercially available bead-based sandwich immune-assay kits ((PDGF AA & BB: Bioassay Technology Laboratory, Shanghai, China; TGF- $\beta$ : Abbkine, CA, USA; BMP-2: Cloud-clone, TA, USA). Standards and samples were assayed in five replicates and mean values were recorded. The detection limit was 5, 2, 15 and 15.6 pg/mL for PDGF-AA, PDGF-BB, TGF- $\beta$  and BMP-2 respectively.

## Osteogenic Differentiation Assay

The osteogenic potential of BMSCs was assessed by osteogenic differentiation assay. Osteogenic induction medium was prepared using  $\alpha$ MEM medium supplemented with 15% FBS, 50 mg/mL L-ascorbate-2-phosphate,  $10^{-7}$  M dexamethasone and 10 mM  $\beta$ -glycerolphosphate. The P2 BMSCs were suspended in  $\alpha$ MEM medium at a density of  $1 \times 10^4$  cells/mL per well and loaded on 24-well plate. After 24 hours, the medium was removed and 1 mL of  $\alpha$ MEM medium or osteogenic medium were added, respectively. The medium was changed every 3 days, for a total culture period of 14 days. To detect calcium deposition, the differentiated BMSCs were fixed with 4% formaldehyde at room temperature for 30 minutes and rinsed rapidly with distilled water. Then, 1 mL of pH 4.2 Alizarin Red S solution (Sigma, St. Louis, USA) was added to cover cell surface for 5 minutes, followed by washing thoroughly with distilled water. The calcium deposits exhibited as orange red sediments on the cell surface and were recorded microscopically.

## Establishment Of Mouse Osteoporotic Model Via Bilateral Ovariectomy

The illustration of mouse bilateral ovariectomy surgical model was shown in Fig. 1a. The female ICR mice (BioLASCO Taiwan Co., Ltd., Taipei, Taiwan) were maintained in polycarbonate cages at  $21 \pm 2$  °C with a 12 hours' light/dark cycle and given access to food and water ad libitum for 4 weeks as an adaptation period. Before surgery, the mice were placed under general anesthesia consisting of an

intramuscular injection (0.25 mL/kg) with 1:1 mixture of Zoletil®50 (Virbac Laboratories, Carros, France) and xylazine (Balanzine®, Health-Tech Pharmaceutical Co., Taiwan). The animals were infiltrated with 1% lidocaine to the incision site to reduce the operative pain. A 1-cm longitudinal incision was made at the intersection which was 0.5 cm from the central spine and 1 cm below the lower rib edge. The ovarian fat pad was lifted and the bilateral ovaries were exteriorized and carefully removed followed by suture ligations to minimize bleeding (Fig. 1b). The abdominal muscles were then closed using an absorbable suture (Vicryl 3.0, ETHICON Inc., Somerville, NJ, USA). The ovariectomized (OVX) mice were then observed twice a day for a total period of 14 days.

## Micro-computed Tomography (micro-ct)

Eight weeks postoperatively, micro-CT was used to evaluate the changes in bone mineral density (BMD) and trabecular bone morphology between non-ovariectomized mice (non-OVX) and ovariectomized mice (OVX). The protocol of micro-CT used in this study was described as follow. The left tibia of animal was harvested and was placed in a custom jig with water and scanned with a SkyScan 1176 MicroCT scanner (SkyScan, Kontich, Belgium) operating at 40 kV, 600  $\mu$ A, 0.3  $\mu$  of rotation step, 0.5 mm A1 filter and 9 mm/pixel of scan resolution. The image slices were reconstructed using the NRecon (v. 1.4.4, Skyscan) software system. The three dimensional (3D) parameters of bone microarchitecture were calculated using CTAn (v.17.0.0, Skyscan) software. For trabecular bone, the proximal tibia was selected for analysis within a conforming volume of interest commencing at the growth plate and extending a further longitudinal distance of 0.5–1.5 mm in the proximal direction to assess site-specific responses to ovariectomy. Microstructural measurements included the percentage of bone volume versus total tissue volume (BV/TV, %), bone mineral density (BMD, g/cm<sup>3</sup>), trabecular number (Tb.N, 1/mm), and trabecular separation (Tb.Sp, mm).

## *In Vivo* intravenous administration of BMSCs and PRFr

Forty-two OVX mice were used for experiment and were allocated into 7 groups. The OVX mice which received no treatment served as control. To evaluate the accumulative effects of PRFr and BMSCs on bone mass, two different treatment groups were compared, known as the single-injection group or quadruple-injection group. PRFr and cell suspension were administrated through tail vein injection using a 26-gauge needle. Basically, in single-injection group, mice received single dose of either 0.6 mL of PRFr,  $3 \times 10^5$  BMSCs or 0.6 mL of PRFr containing  $3 \times 10^5$  of BMSCs. In quadruple-injection group, mice received injection of either 0.6 mL of PRFr,  $3 \times 10^5$  of BMSCs or 0.6 mL of PRFr containing  $3 \times 10^5$  of BMSCs once a week, for four consecutive weeks. Eight weeks after treatment, all the animals were sacrificed and were subjected for micro-CT analysis followed the protocol as previously described.

## Histological Analysis

For histological evaluation, the tibia specimens were decalcified and fixed in 10% buffered formalin for at least 48 hours before routine processing. The samples were then embedded in paraffin and the blocks were cut into serial 5- $\mu$ m thick sections and stained with hematoxylin and eosin (H&E). The specimen sections were examined under light microscopy (Leica, Japan) for evaluation of trabecular changes.

## Statistical analysis

For the quantitative assay, each data point was derived from three independent experiments or an experiment of quadruplicate assay and was presented as mean with standard deviation. All analyses were performed using GraphPad Prism 8.0 analytic software. Statistical significance was set at a  $p$  value of  $< 0.05$ . The data were analyzed using student t-test, and one-way ANOVA followed by post hoc scheffe test and multiple comparisons Dunnett test. The statistical significances among the experimental groups were indicated with asterisks. Groups labeled with asterisk superscript letters, indicate that the statistic difference between the two groups had the  $p$  value less than 0.05, and was considered significantly different.

## Results

### Characterization and osteogenic potential of BMSCs

The BMSCs were cultivated, expanded and cell morphology was closely monitored. Figure 2a show the colony forming units in passage 0 (P0) primary culture with fibroblast-like morphology. The surface markers of BMSCs were characterized by flow cytometry analysis as shown in Fig. 2b. A phenotype of CD44<sup>+</sup> CD90<sup>+</sup> CD34<sup>-</sup> CD45<sup>-</sup> cell surface markers was identified in the P2 BMSCs. To examine the osteogenic capacity of the cells used in this study, the P2 BMSCs were further treated with osteogenic medium for 14 days to test their ability towards osteoblasts. Figure 2c showed that after 14 days of osteogenic induction, the culture dish showed significant reddish precipitation after alizarin red S staining, representing the mineralization of the culture.

### Cytokine Quantification Of Prfr

In general, 0.2 mL of PRFr could be retrieved from 1 mL of whole venous blood after the PRF was left quiescence for 5 hours. The average concentration of PDGF-AA and BB is  $388.88 \pm 51.71$  ng/L and  $174.77 \pm 23.76$  ng/L respectively. For TGF- $\beta$ , the average concentration is  $53.27 \pm 3.46$  ng/L. For BMP-2, the average concentration is  $94.15 \pm 10.9$  pg/mL.

### Changes Of Bmd And Bony Trabecular In Ovariectomized Mice

The differences in bony profile of non-OVX and OVX mice were revealed (Fig. 2c-f). Before experiment, there was no significant difference in body weight among animals in the experimental groups. There was, however, a significant weight gains in OVX mice than non-OVX eight weeks post-operatively, suggesting the initiation of ovariectomized-induced postmenopausal status. Moreover, compared to non-OVX control, OVX mice exhibited reduced BMDs ( $0.12 \pm 0.03 \text{ g/cm}^3$  vs.  $0.05 \pm 0.02 \text{ g/cm}^3$ ;  $p < 0.01$ ), decreased BV/TV ( $10.89 \pm 2.13\%$  vs.  $4.46 \pm 1.35\%$ ;  $p < 0.001$ ), and lower Tb.N ( $1.31 \pm 0.38 \text{ mm}$  vs.  $0.52 \pm 0.1 \text{ mm}$ ;  $p < 0.001$ ), but increased Tb.Sp ( $0.43 \pm 0.05$  vs.  $0.73 \pm 0.06 \text{ mm}$ ;  $p < 0.0001$ ), 8 weeks after surgery. The results indicate that the osteoporosis model has been successfully established.

## Micro-ct Analysis Of Bmd And Bony Trabecular Morphology

Figure 3a-d showed the bony profile of OVX mice which were left untreated ( $n = 6$ ) or received treatments with either PRFr ( $n = 6$ ), BMSCs ( $n = 6$ ), or combined PRFr and BMSCs injections ( $n = 6$ ). The influence of treatment dosages (low dose; single injection or high-dose; quadruple injections) were also evaluated simultaneously. Compared to untreated OVX mice, there was no significant changes to BMD and bone trabeculae could be detected in mice that received low-dose regimen, regardless the content of injection. On the other hand, the results also showed that there was a trend demonstrating an increased bony profile occurred in high-dose treatment groups. Additionally, in mice which received 4 doses of combined PRFr and BMSCs, the BMD, BV/TV, and TB.N increased, and the TB.Sp decreased significantly compared to untreated OVX mice.

## Histological Analysis

Figure. 4 showed the histological images of the tibial bone in all groups stained by H&E. The results showed that the number of bony trabeculae decreased significantly in OVX mice compared to non-OVX mice. No significant changes in trabecular number was found in low-dose (single-injection) groups. In contrast, the trabecular spacing become narrower in OVX-mice treated with high-dose injection of BMSCs and combined PRFr and BMSCs than untreated control. Moreover, the trabecular conjunction points were obviously increased in OVX groups treated with high-dose injection of combined PRFr and BMSCs.

## Discussion

Fragile fractures resulting from osteoporosis are a major cause of morbidity and mortality in elderly patients [25]. In osteoporotic bone, the proportion of fat content in the bone marrow increased remarkably and was shown to be closely linked to a decreased in BMD [26]. The apparent implication of this clinical phenomenon is an inverse relationship between bone marrow adipogenesis and osteogenesis coupling. This important observation was further reinforced by evidence that an increasing number of adipocytes subsequently suppressed bone marrow stem cells (BMSCs) osteogenesis, leading to increased bone resorption and thus overall bone loss [26–29]. Based on these findings, many studies have emphasized the pivotal role of stem cells in osteoporosis pathogenesis since their osteogenic ability would directly

affect in vivo osteogenesis and bone matrix mineralization. From this standpoint, developing stem cell-based therapy to overcome the substantial decline in the number and function of osteogenic cells by means of stem cell transplantation emerge a major research focus in osteoporotic treatment.

The aims of this present study are to evaluate the therapeutic efficacy of BMSCs and PRFr in preventing bone loss in a well-established osteoporotic mouse model. In our previous studies, PRF displayed pronounced stimulatory effects on cell proliferation, chemotaxis, and differentiation [30–32]. Moreover, most of the studies showing a positive role for platelet concentrate in bone regeneration both in vitro and in vivo [14, 15, 21, 26, 33, 34]. Nonetheless, limited reports are available exploring the efficacy of isolated use of BMSCs and PRFr treatments in an osteoporotic model or their combination use in preventing bone loss. In this study, we found that systemically administered combined BMSCs and PRFr could effectively prevent ovariectomy-induced bone mass attenuation. Our data revealed that BMSCs and PRFr might work synergistically when applied in vivo, which may translate into a plausible therapeutic strategy in osteoporosis treatments.

PRF is a second-generation platelet concentrate produced from autologous blood obtained immediately after single-spin centrifugation[17]. Rapid activation of the coagulation cascade and synthesis of thrombin take place when platelets get contact with glass particles of test tube. In this study, PRFr was utilized as the molecular modulator of osteogenesis because it contains a wide spectrum of growth factors such as PDGF, TGF- $\beta$ , BMP-2 and many others that are able to modulate the regenerative process [17, 35–38]. Moreover, many researches have highlighted the supportive role of platelet concentrate in osteogenesis by promoting cell proliferation, chemotaxis, osteogenic differentiation, and extracellular mineralization [15, 21, 26, 33]. In Parsons et al study, platelet concentrate enhances cellular growth of human mesenchymal stem cells and osteogenic marker expressions [15]. Zhang et al also demonstrated that treatment of rabbit bone marrow mesenchymal stem cells with exogenous platelet-rich plasma promoted osteogenic gene expressions, including alkaline phosphatase (ALP), Osteocalcin (OCN) and runt-related transcription factor-2 (RUNX2) [39]. More importantly, PRP could not only promote osteogenesis but also inhibit adipogenesis of pre-adipocytes. The overall enhanced osteogenesis by PRP treatment was observed in Liu et al. study via the simultaneous up-regulation of osteogenic markers (OCN, RUNX2 and osteopontin) and down-regulation of adipogenic marker expressions (PPAR-g2 and leptin) [26]. Collectively, it is reasonable to believe that PRFr represents an ideal molecular modulator for BMSCs osteogenesis. When applied concurrently in vivo, the cytokines originating from PRFr would exert stimulatory effects on BMSCS osteogenic gene and protein expressions thus accelerating new bone formation.

In current study, osteoporosis was induced by bilateral OVX and bone mass attenuation was successfully demonstrated using micro-CT analysis (Fig. 2). Compared to non-OVX mice, a significant reduction in BMD, BV/TV and Tb.N associated with an increased in Tb.Sp were observed in OVX mice at 8 weeks post-operatively, mimicking postmenopausal osteoporosis in women after estrogen withdrawal. Then, osteogenesis-promoting ability of BMSCs and PRFr was investigated in vivo using OVX mice exhibiting osteoporotic changes. Notably, single-injection of either BMSCs, PRFr or their combination did not result

in significant improvement of bony profile in treated mice compared to non-treated control. In contrast, an increasing trend of improved bony profile was observed in mice received high-dose injection of either PRFr, BMSCs and their combinatory use. However, only in mice which had received four times of systemic injection of combined BMSCs and PRFr showing significant improvement of BMD, BV/TV and Tb.N scores compared to non-treated OVX mice. In addition, this treatment regimen appeared to increase the formation of new trabecular bones evidenced by reduced trabecular separation shown in micro-CT and histology. The micro-CT data are quite consistent with the reports while BMSCs or adipose-derived stem cells were administered systemically to prevent bone loss in OVX animals [23, 29, 40, 41]. Moreover, these data also reinforced the notion that PRFr could augment the therapeutic efficacy of BMSC-based therapy for osteoporotic treatment. Additionally, the synergistic effect of PRFr on stem cell osteogenesis is in line with other PRP-related in vivo studies. According to Wei and colleagues, PRP treatment could enhance bone microarchitecture and effectively upregulate osteogenic marker expressions in OVX-induced osteoporotic rats. In their animal model, the combinatory use of PRP and BMSCs significantly promotes healing of osteoporotic bone defects [41].

Our data confirmed the potential of PRFr in augmenting the effects of BMSCs in a preclinical trial with animal model. However, our study has several limitations. First, this preliminary study was conducted to evaluate the capacity of PRFr and BMSCs in promoting bony profile at eight weeks after injections. However, it might be more thorough to observe the imaging and histological differences over different time points. Secondly, biomechanical analysis should be carried out in future to determine the difference in mechanical strength of analyzed bones among different experimental groups.

## **Conclusion**

In conclusion, we have demonstrated that systemic administration of combined BMSCs and PRFr protected against OVX-induced bone mass loss in mice. Moreover, the improvement of bony profile scores in quadruple injection group is better than the single-injection group, probably through the increase in effect size of cells and growth factors. Our data also revealed the combination therapy of BMSCs and PRFr has a synergistic effect in enhancing osteogenesis, which may provide insight for the development of a novel therapeutic strategy in osteoporosis treatment.

## **Abbreviations**

BMD: bone marrow density; BMSC:bone marrow stem cells; BV/TV:bone volume versus total tissue volume; OVX:ovariectomized; PRFr:platelet-rich fibrin releasate; Tb.N:trabecular number; Tb.Sp:trabecular separation.

## **Declarations**

## **Acknowledgment**

Not applicable.

## Author Contributions

C.C.-Wong and J.H.-Liao are responsible for the design of the study and execution of the experiments statistical analysis, and interpretation of the data. S.Y.-Sheu participated in the specimens' processing and histologic evaluation and analysis. P.Y.-Lin participated in the study and in vivo experiments. S.Y.-Sheu and T.F.-Kuo participated in the design of the study and the interpretation of the data, and supervised all of the experiments. All authors read and approved the final manuscript.

## Funding

This study was financially supported in part by grants from the Taiwan Ministry of Science and Technology (MOST103-2313-B-002-040-MY2), and Chung Shan Medical University Hospital (CSH-2020-A-029). This publication was further supported by Research Grants for Newly Hired Faculty (TMU108-AE1-B03) of Taipei Medical University.

## Availability of data and materials

The data analyzed during the current study are available from the corresponding author on reasonable request.

## Ethics Approval

All procedures of bone marrow stem cells isolation and surgery on experimental animals were carried out according to the guide for the Care and Use of Laboratory Animals and was approved by the Institutional Animal Care and Use Committee (IACUC approval: NTU-102-EL-82 and NTU-102-EL-91).

## Consent for publication

Not applicable

## Competing interests

The authors have no conflict of interest to disclose.

## References

1. Tu KN, Lie JD, Wan CKV, Cameron M, Austel AG, Nguyen JK, Van K, Hyun D. Osteoporosis: A Review of Treatment Options. *P t.* 2018;43(2):92–104.
2. Sale JE, Beaton D, Bogoch E. Secondary prevention after an osteoporosis-related fracture: an overview. *Clin Geriatr Med.* 2014;30(2):317–32.
3. Raisz LG. Pathogenesis of osteoporosis: concepts, conflicts, and prospects. *J Clin Invest.* 2005;115(12):3318–25.
4. Karsenty G, Wagner EF. Reaching a genetic and molecular understanding of skeletal development. *Dev Cell.* 2002;2(4):389–406.
5. Rodan GA, Martin TJ. Therapeutic approaches to bone diseases. *Science.* 2000;289(5484):1508–14.
6. Seeman E. Bone quality: the material and structural basis of bone strength. *J Bone Miner Metab.* 2008;26(1):1–8.
7. Seeman E, Delmas PD. Bone quality—the material and structural basis of bone strength and fragility. *N Engl J Med.* 2006;354(21):2250–61.
8. Kharazmi M, Hallberg P, Warfvinge G, Michaelsson K. Risk of atypical femoral fractures and osteonecrosis of the jaw associated with alendronate use compared with other oral bisphosphonates. *Rheumatology.* 2014;53(10):1911–3.
9. McClung M, Harris ST, Miller PD, Bauer DC, Davison KS, Dian L, Hanley DA, Kendler DL, Yuen CK, Lewiecki EM. Bisphosphonate therapy for osteoporosis: benefits, risks, and drug holiday. *Am J Med.* 2013;126(1):13–20.
10. Wirth SM, Lawson AP, Sutphin SD, Adams VR. Osteonecrosis of the jaw associated with bisphosphonate therapy. *Orthopedics.* 2009;32(12):900.
11. Teitelbaum SL. Stem cells and osteoporosis therapy. *Cell Stem Cell.* 2010;7(5):553–4.
12. Tokuzawa Y, Yagi K, Yamashita Y, Nakachi Y, Nikaido I, Bono H, Ninomiya Y, Kanesaki-Yatsuka Y, Akita M, Motegi H, et al. Id4, a new candidate gene for senile osteoporosis, acts as a molecular switch promoting osteoblast differentiation. *PLoS Genet.* 2010;6(7):e1001019.
13. Wang C, Meng H, Wang X, Zhao C, Peng J, Wang Y. Differentiation of Bone Marrow Mesenchymal Stem Cells in Osteoblasts and Adipocytes and its Role in Treatment of Osteoporosis. *Med Sci Monit.* 2016;22:226–33.
14. Uggeri J, Belletti S, Guizzardi S, Poli T, Cantarelli S, Scandroglio R, Gatti R. Dose-dependent effects of platelet gel releasate on activities of human osteoblasts. *J Periodontol.* 2007;78(10):1985–91.
15. Parsons P, Butcher A, Hesselden K, Ellis K, Maughan J, Milner R, Scott M, Alley C, Watson JT, Horner A. Platelet-rich concentrate supports human mesenchymal stem cell proliferation, bone morphogenetic protein-2 messenger RNA expression, alkaline phosphatase activity, and bone formation in vitro: a mode of action to enhance bone repair. *J Orthop Trauma.* 2008;22(9):595–604.
16. Man Y, Wang P, Guo Y, Xiang L, Yang Y, Qu Y, Gong P, Deng L. Angiogenic and osteogenic potential of platelet-rich plasma and adipose-derived stem cell laden alginate microspheres. *Biomaterials.* 2012;33(34):8802–11.

17. Dohan DM, Choukroun J, Diss A, Dohan SL, Dohan AJ, Mouhyi J, Gogly B. Platelet-rich fibrin (PRF): a second-generation platelet concentrate. Part I: technological concepts and evolution. *Oral Surg Oral Med Oral Pathol Oral Radiol Endod.* 2006;101(3):e37–44.
18. Dohan DM, Choukroun J, Diss A, Dohan SL, Dohan AJ, Mouhyi J, Gogly B. Platelet-rich fibrin (PRF): a second-generation platelet concentrate. Part II: platelet-related biologic features. *Oral Surg Oral Med Oral Pathol Oral Radiol Endod.* 2006;101(3):e45–50.
19. Dohan DM, Choukroun J, Diss A, Dohan SL, Dohan AJ, Mouhyi J, Gogly B. Platelet-rich fibrin (PRF): a second-generation platelet concentrate. Part III: leucocyte activation: a new feature for platelet concentrates? *Oral Surg Oral Med Oral Pathol Oral Radiol Endod.* 2006;101(3):e51–5.
20. Kobayashi M, Kawase T, Horimizu M, Okuda K, Wolff LF, Yoshie H. A proposed protocol for the standardized preparation of PRF membranes for clinical use. *Biologicals.* 2012;40(5):323–9.
21. Kosmacheva SM, Danilkovich NN, Shchepen AV, Ignatenko SI, Potapnev MP. Effect of platelet releasate on osteogenic differentiation of human mesenchymal bone marrow stem cells. *Bull Exp Biol Med.* 2014;156(4):560–5.
22. Dutta S, Sengupta P. Men and mice: Relating their ages. *Life Sci.* 2016;152:244–8.
23. Rocha MAC, Silva LMC, Oliveira WA, Bezerra DO, Silva GCD, Silva LDS, Medeiros B, Baeta SAF, Carvalho MAM, Argolo NMN. Allogeneic mesenchymal stem cells and xenogenic platelet rich plasma, associated or not, in the repair of bone failures in rabbits with secondary osteoporosis. *Acta Cir Bras.* 2017;32(9):767–80.
24. Su CY, Kuo YP, Tseng YH, Su CH, Burnouf T. In vitro release of growth factors from platelet-rich fibrin (PRF): a proposal to optimize the clinical applications of PRF. *Oral Surg Oral Med Oral Pathol Oral Radiol Endod.* 2009;108(1):56–61.
25. Compston JE, McClung MR, Leslie WD. **Osteoporosis** *Lancet.* 2019;393(10169):364–76.
26. Liu HY, Wu AT, Tsai CY, Chou KR, Zeng R, Wang MF, Chang WC, Hwang SM, Su CH, Deng WP. The balance between adipogenesis and osteogenesis in bone regeneration by platelet-rich plasma for age-related osteoporosis. *Biomaterials.* 2011;32(28):6773–80.
27. Muschler GF, Nitto H, Boehm CA, Easley KA. Age- and gender-related changes in the cellularity of human bone marrow and the prevalence of osteoblastic progenitors. *J Orthop Res.* 2001;19(1):117–25.
28. Sethe S, Scutt A, Stolzing A. Aging of mesenchymal stem cells. *Ageing Res Rev.* 2006;5(1):91–116.
29. Antebi B, Pelled G, Gazit D. Stem cell therapy for osteoporosis. *Curr Osteoporos Rep.* 2014;12(1):41–7.
30. Wong CC, Chen CH, Chan WP, Chiu LH, Ho WP, Hsieh FJ, Chen YT, Yang TL. Single-Stage Cartilage Repair Using Platelet-Rich Fibrin Scaffolds With Autologous Cartilaginous Grafts. *Am J Sports Med.* 2017;45(13):3128–42.
31. Wong CC, Kuo TF, Yang TL, Tsuang YH, Lin MF, Chang CH, Lin YH, Chan WP. **Platelet-Rich Fibrin Facilitates Rabbit Meniscal Repair by Promoting Meniscocytes Proliferation, Migration, and Extracellular Matrix Synthesis.** *Int J Mol Sci* 2017, 18(8).

32. Wong CC, Ou KL, Lin YH, Lin MF, Yang TL, Chen CH, Chan WP. **Platelet-Rich Fibrin Facilitates One-Stage Cartilage Repair by Promoting Chondrocytes Viability, Migration, and Matrix Synthesis.** *International journal of molecular sciences* 2020, 21(2).
33. Sharif PS, Abdollahi M. The role of platelets in bone remodeling. *Inflamm Allergy Drug Targets*. 2010;9(5):393–9.
34. Zou J, Yuan C, Wu C, Cao C, Yang H. The effects of platelet-rich plasma on the osteogenic induction of bone marrow mesenchymal stem cells. *Connect Tissue Res*. 2014;55(4):304–9.
35. Foster TE, Puskas BL, Mandelbaum BR, Gerhardt MB, Rodeo SA. Platelet-rich plasma: from basic science to clinical applications. *Am J Sports Med*. 2009;37(11):2259–72.
36. Jalowiec JM, D'Este M, Bara JJ, Denom J, Menzel U, Alini M, Verrier S, Herrmann M. An In Vitro Investigation of Platelet-Rich Plasma-Gel as a Cell and Growth Factor Delivery Vehicle for Tissue Engineering. *Tissue Eng Part C Methods*. 2016;22(1):49–58.
37. Kang YH, Jeon SH, Park JY, Chung JH, Choung YH, Choung HW, Kim ES, Choung PH. Platelet-rich fibrin is a Bioscaffold and reservoir of growth factors for tissue regeneration. *Tissue Eng Part A*. 2011;17(3–4):349–59.
38. Khiste SV, Naik Tari R. Platelet-Rich Fibrin as a Biofuel for Tissue Regeneration. *ISRN Biomaterials*. 2013;2013:1–6.
39. Zhang M, Zhen J, Zhang X, Yang Z, Zhang L, Hao D, Ren B. Effect of Autologous Platelet-Rich Plasma and Gelatin Sponge for Tendon-to-Bone Healing After Rabbit Anterior Cruciate Ligament Reconstruction. *Arthroscopy*. 2019;35(5):1486–97.
40. Cho HS, Song IH, Park SY, Sung MC, Ahn MW, Song KE. Individual variation in growth factor concentrations in platelet-rich plasma and its influence on human mesenchymal stem cells. *Korean J Lab Med*. 2011;31(3):212–8.
41. Wei B, Huang C, Zhao M, Li P, Gao X, Kong J, Niu Y, Huang R, Quan J, Wei J, et al. Effect of Mesenchymal Stem Cells and Platelet-Rich Plasma on the Bone Healing of Ovariectomized Rats. *Stem cells international*. 2016;2016:9458396.

## Figures

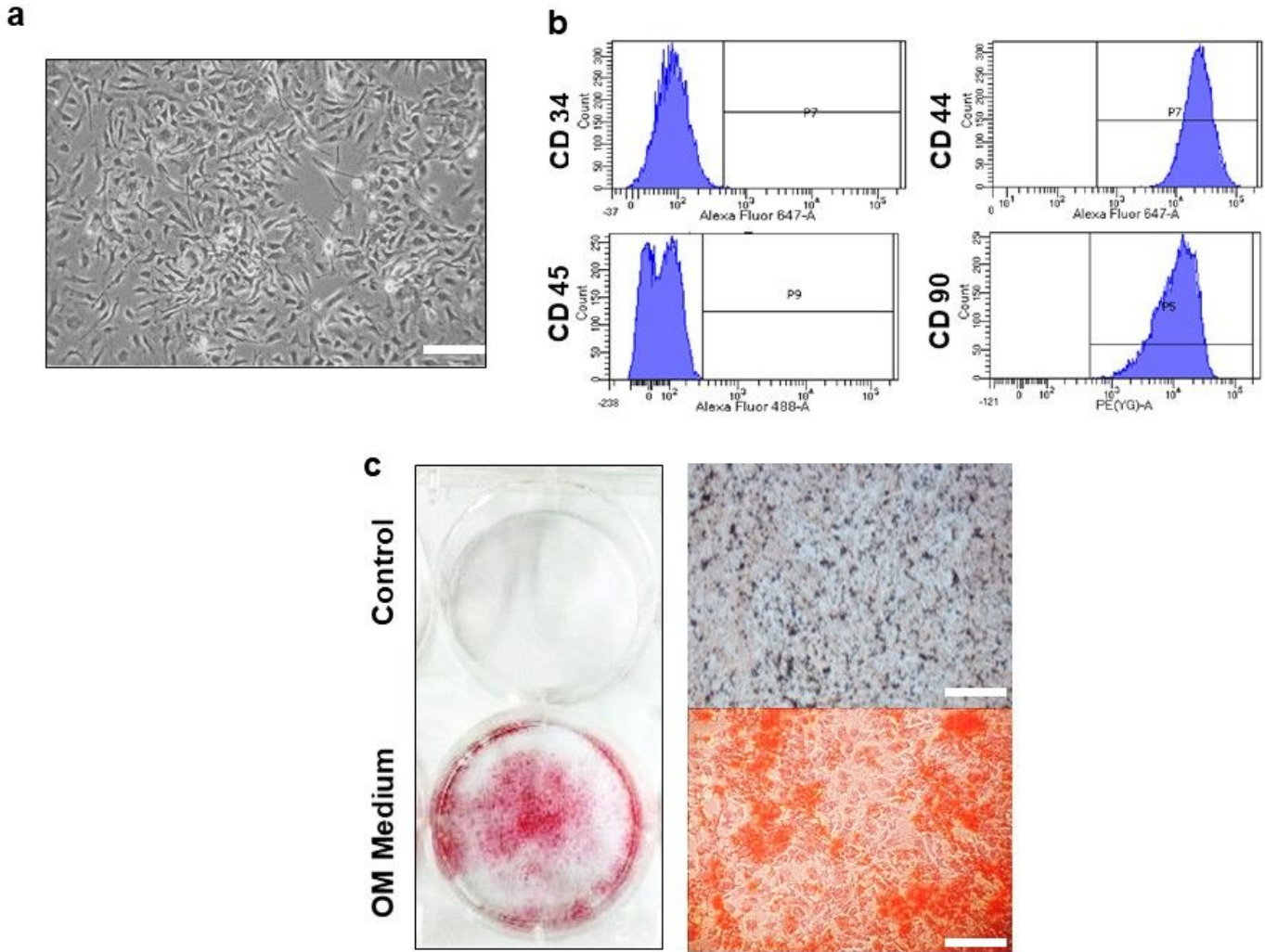


**Figure 1**

Cell morphology, surface marker expressions and osteogenic differentiation potential of bone marrow stem cells (BMSCs). (a) Colony forming unit is shown under bright field observation in the passage 0 BMSC culture. (b) For flow cytometry analysis, the BMSCs were found to exhibit a phenotype of CD44+ CD90+ CD34- CD45-. (c) Alizarin Red S staining of BMSCs cultured in standard medium (upper panel) or osteogenic differentiation medium (lower panel) for 14 days. Scale bar- 100  $\mu$ m.

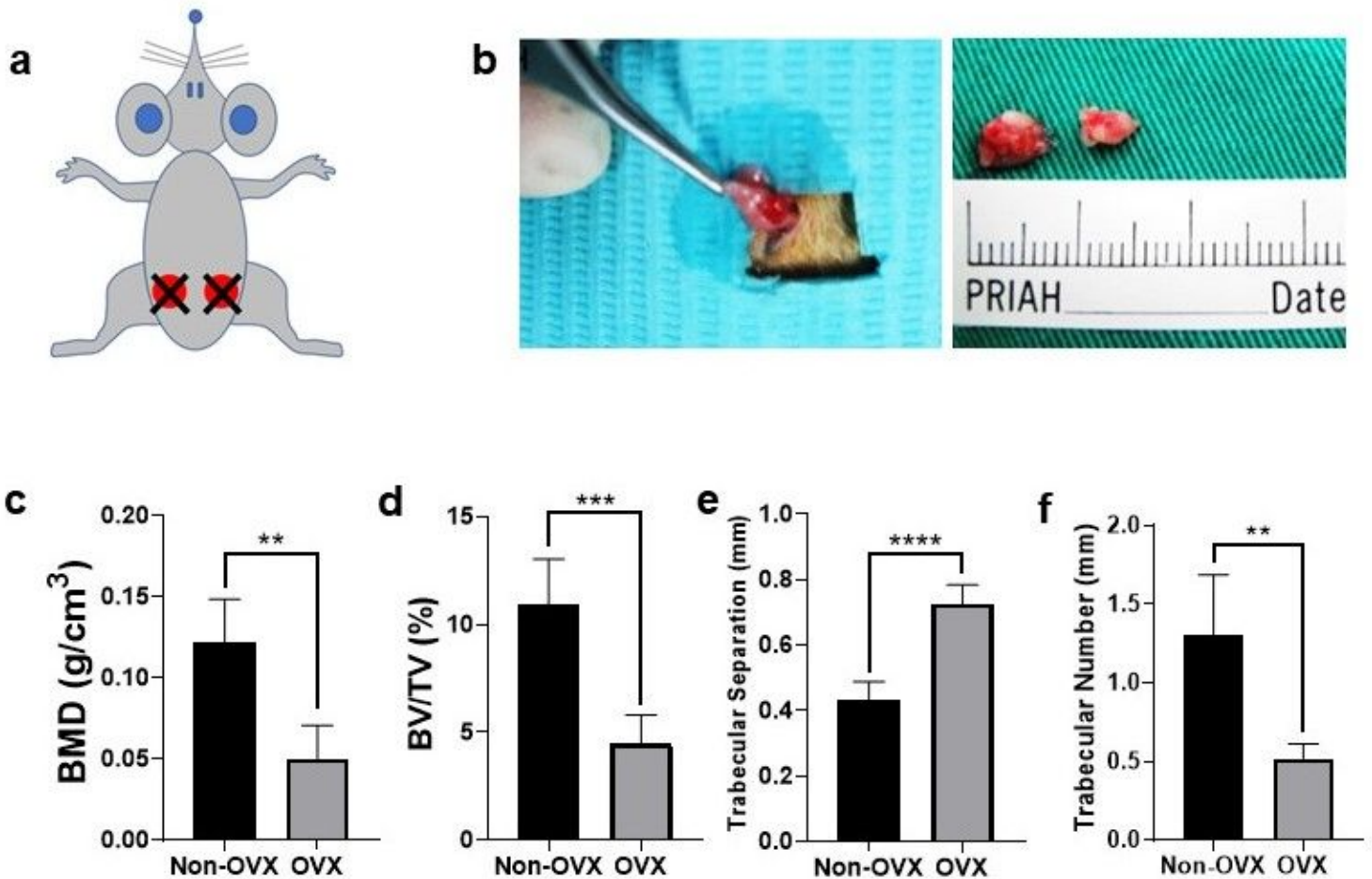


**Figure 2**

(a) Schematic illustration of osteoporotic mouse model created by bilateral ovariectomy. (b) The ovary with the associated fat pad is gently withdrawn using sterile blunt forceps. Bilateral ovaries were removed after suture ligation. (c) Micro-CT analysis of bone marrow density (BMD), bone volume versus total tissue volume (BV/TV, %), trabecular number (Tb.N), and trabecular separation (Tb.Sp) in non-ovariectomized (Non-OVX) and ovariectomized (OVX) mice eight weeks after surgery. The bars show the mean  $\pm$  SD (n = 6) of each group. \*\*P< .01; \*\*\*P<.001; \*\*\*\*P<.0001.

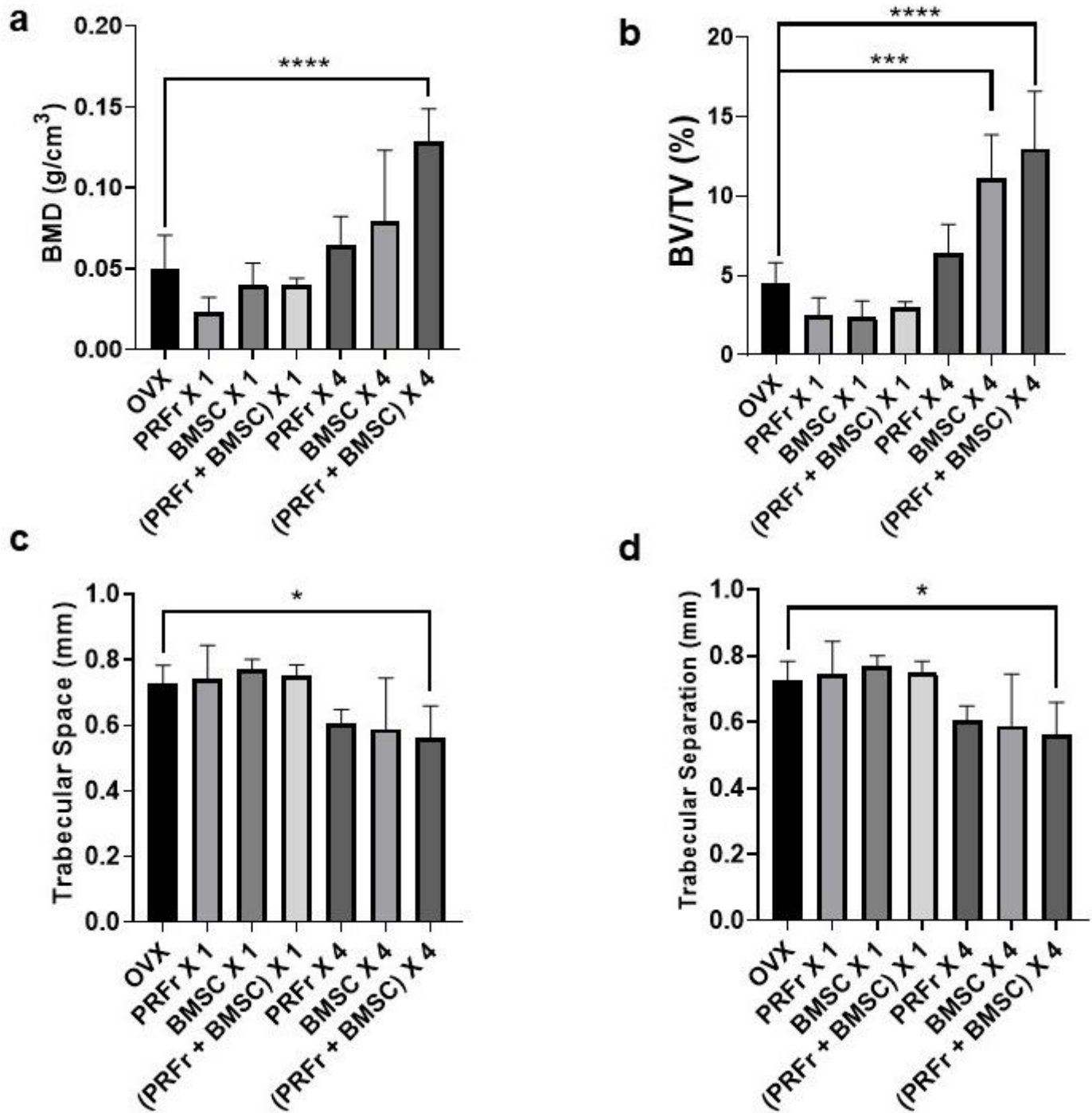


**Figure 3**

Micro-CT analysis of ovarietomized mice in untreated control (OVX), or experimental groups which received injection with either platelet-rich fibrin releasate (PRFr), bone marrow stem cells (BMSC) or in combination therapy (PRFr + BMSC). Low-dose group received single injection (X 1) while the high-dose group received quadruple injections (X 4). The bone marrow density (BMD), bone volume versus total tissue volume (BV/TV, %), trabecular number (Tb.N), and trabecular separation (Tb.Sp) in each group of mice were evaluated 8-weeks after injection. The bars show the mean  $\pm$  SD (n = 6) of each group. \*P< .05; \*\*\*P<.001; \*\*\*\*P<.0001.

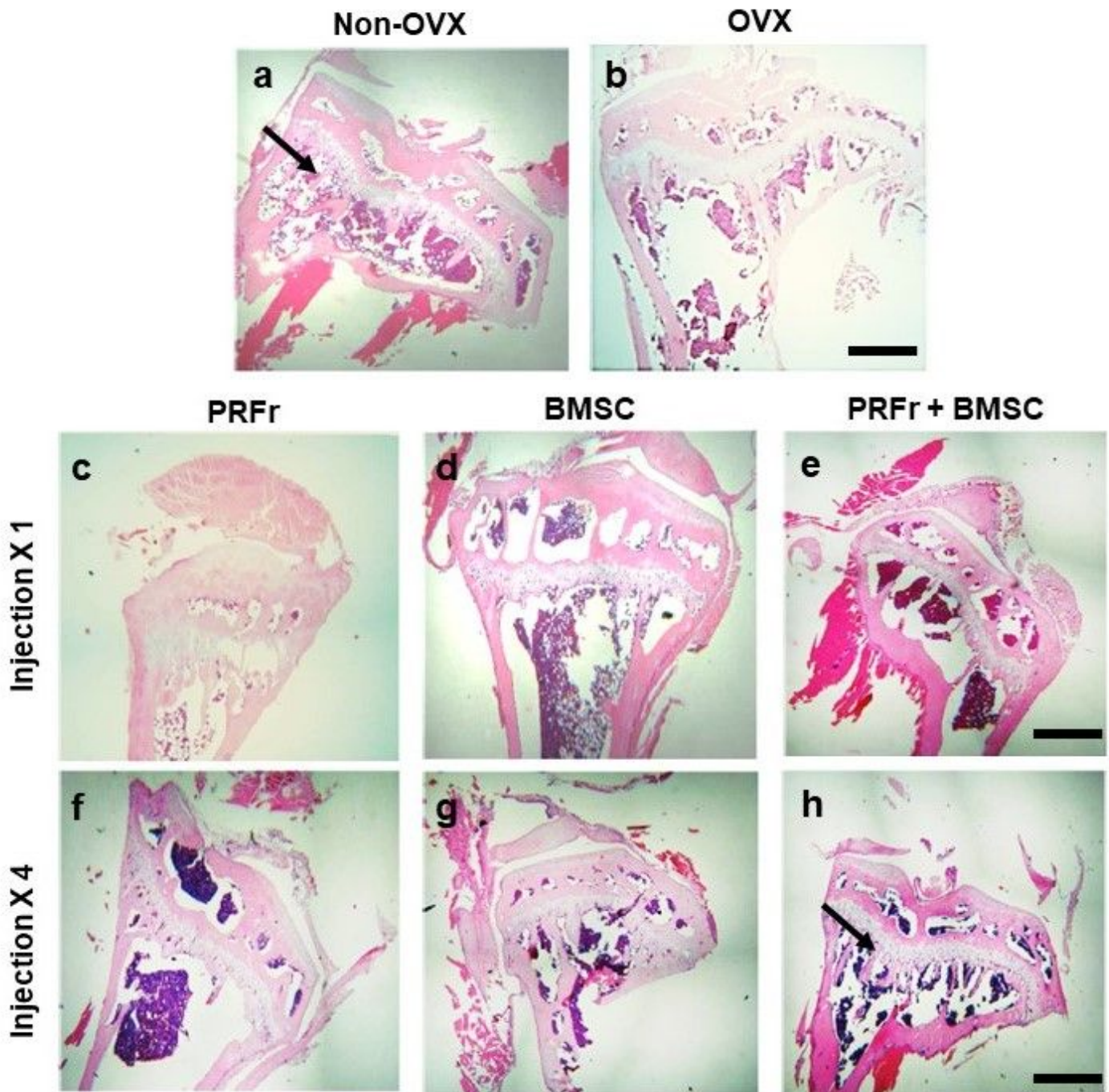


**Figure 4**

Histological sections of proximal tibial bony architecture in non-ovariectomized (Non-OVX) mice (a) and ovariectomized (OVX) mice (b) stained by hematoxylin and eosin (H&E). (c-e) Proximal tibial sections from mice received intravenous injection of either platelet-rich fibrin releasate (PRFr), bone marrow stem cells (BMSC) or in combination therapy (PRFr + BMSC). Low-dose group received single injection (X 1) while the high-dose group received quadruple injections (X 4). The black arrows indicate bony trabeculae. Scale bar- 2.5 mm.

## Supplementary Files

This is a list of supplementary files associated with this preprint. Click to download.

- [20200508ARRIVEguidelines.docx](#)